International Journal of Pharmaceutics 397 (2010) 194–200

Contents lists available at ScienceDirect

International Journal of Pharmaceutics

journal homepage: www.elsevier.com/locate/ijpharm

Pharmaceutical Nanotechnology

Preparation, characterization, and biodistribution of letrozole loaded PLGA nanoparticles in Ehrlich Ascites tumor bearing mice

Nita Mondal[a], Kamal Krishna Halder[b], Madan Mohan Kamila[a], Mita Chatterjee Debnath[b,*], Tapan K. Pal[a], Saroj K. Ghosal[a], Bharat R. Sarkar[c], Shantanu Ganguly[c]

[a] Division of Pharmaceutics, Department of Pharmaceutical Technology, Jadavpur University, Kolkata 700032, India
[b] Nuclear Medicine Division, Indian Institute of Chemical Biology (CSIR), 4, Raja S.C. Mullick Road, Jadavpur, Kolkata 700032, India
[c] Regional Radiation Medicine Centre, Thakurpukur Cancer Centre and Welfare Home Campus, Kolkata, India

ARTICLE INFO

Article history:
Received 8 March 2010
Received in revised form 23 June 2010
Accepted 28 June 2010
Available online 6 July 2010

Keywords:
Letrozole
Technetium-99m
PLGA nanoparticles
Biodistribution
Tumor uptake

ABSTRACT

Letrozole (LTZ) incorporated PLGA nanoparticles were prepared by solvent displacement technique and characterized by transmission electron microscopy, poly-dispersity index and zeta potential measurement. Radiolabeling of free LTZ and LTZ-loaded PLGA NPs was performed with technetium-99m with high labeling efficiency. The labeled complex showed good in vitro stability as verified by DTPA challenge test. The labeled complexes also showed significant in vivo stability when incubated in rat serum for 24 h. Biodistribution studies of ^{99m}Tc-labeled complexes were performed after intravenous administration in normal mice and Ehrlich Ascites tumor bearing mice. Compared to free LTZ, LTZ-loaded PLGA NPs exhibited significantly lower uptake by the organs of RES. The tumor concentration of LTZ-loaded PLGA NPs was 4.65 times higher than that of free LTZ at 4 h post-injection. This study indicates the capability of PLGA nanopartcles in enhancing the tumor uptake of letrozole.

1. Introduction

In recent years nanotechnology, as applied to medicine, has brought significant advances in the diagnosis and treatment of diseases. Nanoparticles (NPs) are considered to be the best drug delivery system, have considerable potential for drug targeting and exhibit several advantages over conventional delivery systems (Hughes, 2005; Allemann et al., 1993). These are: high stability conferring long shelf lives, high carrier capacity, feasibility of incorporation of both hydrophilic and hydrophobic substances, and possibility of administration through variable routes (Allen et al., 1993). Nanoparticles can also be designed to allow controlled drug release from the matrix. All these properties enable improvement of drug bioavailability producing high level of pharmacological action and reduction of the dosing frequency (Soppimath et al., 2001). Drugs incorporated into nanoparticles can be targeted to a specific site of action with concomitant reduction in the quantity of drug required and dosage toxicity, enabling safe delivery of toxic therapeutic drugs as well as protection of non-target tissues and cells from severe side effects (Brannon-Peppas, 1995).

Breast cancer is the most common non-cutaneous cancer among women. It is the second leading cause of cancer-related deaths in the United States (Weir et al., 2003). The antiestrogen tamoxifen has long been used in the treatment of pre- and postmenopausal breast cancer (Vogel, 2001). However some breast cancer became resistant to tamoxifen, and in some cases the drug increases the risk of endometrial cancer (Brown, 2002). Nowadays the aromatase inhibitors, representing a new class of agents are considered as more effective than tamoxifen in the treatment of breast cancer (Miller, 1997). Letrozole (LTZ) is an oral non-steroidal aromatase inhibitor approved by United States FDA and has been introduced for the adjuvant treatment of hormonally responsive local or metastatic breast cancer (Cohen et al., 2002; Long et al., 2004). It decreases the amount of estrogen produced by the body and can slow or stop the growth of some breast tumors that need estrogen to grow. LTZ-loaded nanoparticulate formulation has been developed to facilitate controlled release and targeted delivery of drugs thereby enhancing its therapeutic efficacy.

Polymeric nanoparticles have recently been considered as promising carriers for anticancer agents (Brigger et al., 2002; Vauthier et al., 2003). Poly-D,L-lactic-co-glycolic acid (PLGA), a copolymer of lactic and glycolic acids, is an excellent synthetic non-toxic biodegradable copolymer (Jain, 2000). It has been widely applied to formulate hydrophobic as well as hydrophilic drugs into nanoparticulate delivery systems because of its excellent biocompatibility, biodegradability and bioresorbability. Incorporation

* Corresponding author. Tel.: +91 33 2473 3491; fax: +91 33 2473 5197/+91 33 2472 3967.
E-mail addresses: mitacd@iicb.res.in, mita_chdebnath@yahoo.com (M.C. Debnath).

0378-5173/$ – see front matter © 2010 Elsevier B.V. All rights reserved.
doi:10.1016/j.ijpharm.2010.06.049

of drugs into PLGA based nanoparticulate formulation results in significant change in tissue distribution profile, target specificity and pharmacokinetic behaviour (Yamaguchi and Anderson, 1993; Mainardes and Evangelista, 2005; Dillen et al., 2006). As these nanoparticles are small enough they are expected to circulate through capillaries, cross the highly permeable vasculature supplying blood to tumor (angiogenetic area), and enter tumor cells through endocytosis (Jin et al., 2008). All these may lead to improved therapeutic efficacy, better use of the drug, increased patient compliance and improved quality of life.

The objective of this study is to evaluate the biodistributive properties of free LTZ and LTZ-loaded PLGA NPs in mice bearing Ehlrich Ascites tumor and to investigate the capability of PLGA nanoparticles to enhance the tumor uptake of letrozole. LTZ-loaded PLGA NPs were prepared by solvent displacement technique using poloxamer-188 as stabilizer with slight modifications of the reported method (Mondal et al., 2008). Poloxamer-188 was used as surfactant to keep the precipitated particles suspended and discrete. Incorporation of poloxamer-188 in nanoparticulate formulation resulted in significant enhancement of the cytotoxic effect of the anticancer drug (Yan et al., 2010). The free drug (LTZ), and the LTZ-loaded PLGA NPs were radiolabeled with technetium-99m by direct radiolabeling approach using stannous chloride dihydrate as reductant. ^{99m}Tc-labeled LTZ and LTZ-loaded PLGA NPs were intravenously administered to normal and EA tumor bearing mice. Biodistributions in various organs, tumor uptake and retention were evaluated. The results are discussed in the following section.

2. Materials and methods

2.1. Chemicals

Poly-D,L-lactic-co-glycolic acid (PLGA), with a copolymer ratio of D,L-lactide to glycolide of 50:50 (Resomer 503H, average molecular weight 33,000 Da) and with inherent viscosity 0.32–0.44 dl/g, was purchased from Boehringer Ingelheim Co. (Ingelheim, Germany). Diethylene triamine pentaacetic acid (DTPA) and stannous chloride dihydrate were purchased from Sigma Chemical Co. (USA). Letrozole and poloxamer-188 (Lutrol 68) were gifted by Sun Pharmaceuticals Advanced Research Center (Baroda, Gujarat, India) and Ranbaxy Research Laboratory (Guragaon, India), respectively. $^{99}MoO_4^-$ was purchased from the Bhabha Atomic Research Centre (Mumbai) and $^{99m}TcO_4^-$ was obtained by 2-butanone extraction of a 5(N) NaOH solution of $^{99}MoO_4^-$. All other chemicals and solvents were of analytical grade and purchased from Merck India.

2.2. Preparation of letrozole loaded PLGA nanoparticles

The nanoparticles loaded with letrozole (LTZ) were prepared by solvent displacement technique as per the reported method (Mondal et al., 2008) with some alteration. Briefly a solution of 150 mg of PLGA (50:50) in 5 ml of acetone containing 50 mg of letrozole (drug polymer ratio 1:3) was added to an aqueous phase containing 0.5–1% (w/v) poloxamer-188 at a constant flow rate (0.3 ml/min) under mechanical stirring at 2000 rpm. The organic phase was evaporated at room temperature with constant stirring for 5 h. Finally the nanoparticles were isolated by centrifugation at 10,000 × g at 4 °C for 30 min and washed twice with double distilled water to remove free LTZ. The washings were discarded by centrifugation as described above. The suspension was then lyophilized (VIRTIS, Freeze Mobile, Model-6ES, Cambridge, USA) for 48 h using glucose and lactose (in the ratio of NPs:gluc:lact: 1:0.667:1.333 (w/w)) as lyoprotectant and cryoprotectant, respectively to obtain dry powdered nanoparticles.

2.3. Characterization of nanoparticles

LTZ-loaded PLGA NPs were characterized by different physicochemical methods. Both morphology and particle size distribution of nanoparticles were determined by transmission electron microscopy (TEM) on TECNAI SPIRIT model FE1 electron microscope (The Netherlands) as per reported protocol (Halder et al., 2008). Particle size distribution was also analysed by master sizer 2000 (Malvern instruments, UK). The polydispersity index of NPs was estimated by photon correlation spectroscopy (Zetasizer Nano ZS, Malvern, UK) at a fixed angle of 90°. Samples were diluted with dust-free water to give the recommended scattering intensity. Analysis was carried at least for three times for each batch of sample and mean values were reported.

The particle charge of LTZ-loaded PLGA NPs was quantified by measurement of zeta potential by laser Doppler anmometry in Zetasizer Nano ZS (Malvern, UK). Samples were diluted with distilled water. The frequency shift or phase shift of an incident laser beam caused by these moving particles is measured as particle mobility, which is converted to zeta potential by the application of the Smoluchowski or Huckel theories.

The drug content of LTZ-loaded PLGA NPs was determined by centrifuging (25,000 rpm) the nano-dispersion at 4 °C for 1 h (Mondal et al., 2008). The residue was washed twice with distilled water and dried in vacuum. The yield was calculated based on the weight of the dry powder yield. The amount of entrapped letrozole in nano-dispersion was determined spectrophotometrically (UV-2450, Shimadzu, Japan) by shaking a known amount of nanoparticles in measured volume of methanol for 2 h and measuring the optical density (at 238 nm) of the entrapped drug present in the filtrate.

2.4. Radiolabeling of letrozole and letrozole loaded PLGA nanoparticles

LTZ and LTZ-loaded PLGA NPs were radiolabeled with technetium-99m (^{99m}Tc) by reduction with stannous chloride dihydrate as per the reported method (Richardson et al., 1977; Halder et al., 2008) with some modifications. Briefly aqueous $^{99m}TcO_4^-$ (74–148 MBq) was added either to aqueous solution of LTZ (1.8 mg/ml; pH adjusted to 4.0 with 0.05 N NaOH) or to drug loaded nanoparticles (equivalent to 1.8 mg/ml of letrozole; pH 4.0), this was followed by the addition of freshly prepared stannous chloride dihydrate solution (20 μl containing 20 μg of $SnCl_2$) to each and incubation for 15 min. Final pH of the reaction mixture was 3.75. The labeling efficiencies of LTZ and LTZ-loaded PLGA NPs were determined by ascending thin layer chromatography (TLC) using 2.5 cm × 10 cm silica gel strips (Merck Germany) as stationary phase and either acetone or ethanol: water (7:3) as mobile phase. The plates were developed after spotting the plates with test samples (2–3 μl) and quantitative analyses of the chromatograms were performed by cutting the strips into 1 cm pieces and counting them in a well-type gamma scintillation counter (Electronic Corporation of India Model LV4755, Hyderabad, India) at 140 keV.

2.5. Stability studies

In vitro stability of the ^{99m}Tc-labeled complexes of LTZ and LTZ-loaded PLGA NPs in 0.9% sodium chloride and serum was determined by ascending TLC technique. The labeled complex (0.5 ml) was mixed with 1.5 ml of normal saline or rat serum and incubated at 37 °C. The samples were withdrawn at regular intervals upto 24 h to monitor the stability by TLC.

2.6. DTPA challenge

This study was performed to check the stability and strength of binding of ^{99m}Tc with the drug loaded nanoparticles. Aliquots (0.5 ml) of the radiolabeled preparations were challenged against three different concentrations (10, 30, and 50 mM) of DTPA in 0.9% saline by incubating at 37 °C for 2 h. The effect of DTPA on labeling was measured by thin layer chromatography on silica gel plates using acetone and normal saline separately as mobile phase that allowed the separation of free pertechnetate (R_f = 0) and DTPA-chelate (R_f = 0.9) from that of the ^{99m}Tc-labeled LTZ-loaded PLGA NPs which remains at the point of application (R_f = 0).

2.7. Tumor implantation

Ehrlich Ascites tumor (EAT) cells were maintained in the peritoneum of Swiss albino mice in the Ascites form by serial weekly passage. Exponentially growing cells were harvested, washed and resuspended in saline and ~2×10^7 cells were injected intramuscularly in the thigh of the right hind leg of the mice. After 12–14 days, a palpable tumor in the volume range of 1 ± 0.1 cm^3 was observed and used for further studies.

2.8. Biodistribution studies

All animal experiments were approved by the Social Justice and Empowerment Committee for the purpose of control and supervision of experiments on animals (CPCSEA), Government of India, New Delhi. Biodistribution studies were performed in normal Swiss albino mice (25–30 g) as well as in tumor model. All animals were well hydrated by intraperitoneal administration of saline (0.9%, 2 ml) for 1 h. After another 1 h, ^{99m}Tc-chelate of free LTZ or LTZ-loaded PLGA NPs in a total volume 0.03 ml (8–12 MBq/kg) was injected in each mouse through the tail vein. The mice were sacrificed at 1, 4, 8 and 24 h post-injection, desired organs were collected after dissection, washed with normal saline, made free from adhering tissues, and transferred into counting vials. The urinary bladder was clamped, dissected and carefully transferred into counting vials. Blood samples were obtained by puncture of the heart and it was assumed that the blood weight was 7% of the body mass. The samples were counted against suitable diluted aliquots of the injected solution as standard and the results were expressed either as percent dose/g of tissue or percent dose/organ.

2.9. Tumor imaging by gamma scintigraphy

^{99m}Tc-labeled LTZ and LTZ-loaded PLGA NPs (3.7–4.5 MBq) were injected via tail vein to well-hydrated normal and tumor bearing mice. Scintigraphic studies were performed under GE Infinia Gamma Camera equipped with Xeleris Work Station, static images were acquired at 4 h post-injection.

2.10. Statistical analysis

The p-values of the experimental results were calculated and found to be <0.05 (statistically significant).

3. Results

LTZ-loaded PLGA NPs were prepared by solvent displacement technique (Fig. 1). To prevent aggregation, the internal phase, acetone from the nano-dispersion was evaporated by slow stirring at room temperature instead of quick rotative evaporation under partial vacuum. Which yielded spherical powder particles (Fig. 2) with diameter of 15–100 nm and polydispersity index of 0.087 ± 0.019. The value of polydispersity index indicates the narrow distribution

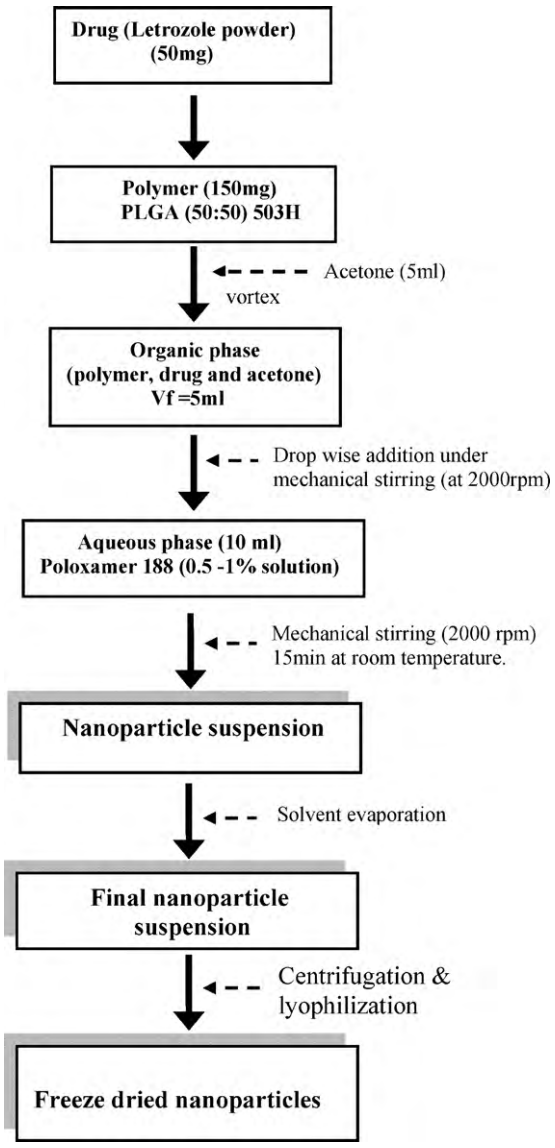

Fig. 1. Diagrams of the methodology and experimental conditions to prepare nanoparticle formulation

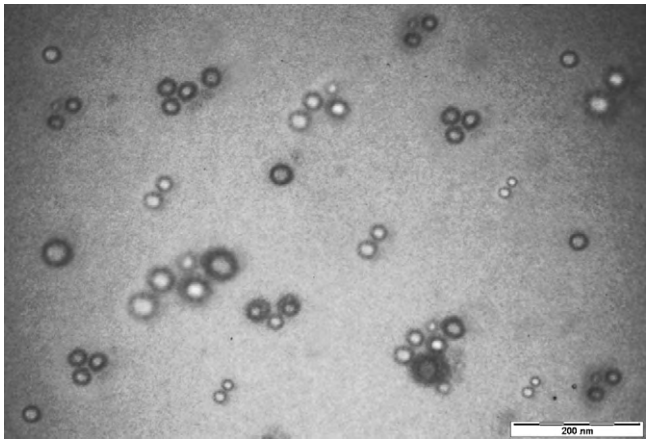

Fig. 2. Transmission electron micrograph of letrozole loaded nanoparticles.

Table 1
Effect of pH on the labeling efficiency of LTZ and LTZ-loaded PLGA NPs.

pH	LTZ			LTZ-loaded PLGA NPs		
	% Colloid	% Labeled	% Free	% Colloid	% Labeled	% Free
3.00	20.10 ± 0.65	73.36 ± 0.46	6.53 ± 0.59	16.59 ± 0.26	78.08 ± 0.36	5.36 ± 0.32
3.50	9.65 ± 0.18	87.66 ± 0.57	3.01 ± 0.20	12.49 ± 0.37	85.13 ± 0.39	2.38 ± 0.22
3.75	5.37 ± 0.28	93.05 ± 0.39	1.58 ± 0.35	4.70 ± 0.24	94.00 ± 0.37	1.30 ± 0.23
4.00	10.67 ± 0.24	85.15 ± 0.59	4.08 ± 0.23	12.70 ± 0.13	84.86 ± 0.26	2.44 ± 0.14
4.25	16.59 ± 0.45	77.11 ± 0.68	6.29 ± 0.38	15.13 ± 0.23	78.90 ± 0.29	6.03 ± 0.07
4.50	39.04 ± 0.77	56.43 ± 1.06	4.59 ± 0.48	27.92 ± 0.84	67.73 ± 0.86	4.34 ± 0.33

Each value is the mean (±SD) of four results.

Table 2
Influence of the amount of stannous chloride on the labeling efficiency of LTZ and LTZ-loaded PLGA NPs. Each value is the mean(± SD)of four results.

$SnCl_2, 2H_2O$ (μg /ml)	LTZ			LTZ-loaded PLGA NPs		
	% Colloid	% Labeled	% Free	% Colloid	% Labeled	% Free
5	2.08 ± 0.13	78.09 ± 1.11	19.83 ± 1.01	2.18 ± 0.19	81.69 ± 1.19	16.13 ± 1.17
10	4.78 ± 0.32	81.18 ± 1.32	14.04 ± 0.91	4.68 ± 0.35	82.21 ± 1.10	13.11 ± 0.97
15	8.72 ± 0.87	87.06 ± 1.90	4.22 ± 0.56	9.17 ± 0.78	84.78 ± 1.01	6.05 ± 0.53
20	5.46 ± 0.12	93.12 ± 0.88	1.42 ± 0.31	5.2 ± 0.90	93.5 ± 0.91	1.3 ± 0.13
30	12.46 ± 1.53	81.08 ± 1.12	6.46 ± 0.19	13.18 ± 1.01	82.21 ± 0.53	4.61 ± 0.33
40	19.83 ± 1.72	72.12 ± 2.11	8.05 ± 0.12	20.19 ± 1.15	73.63 ± 0.37	6.18 ± 0.12

profile of particles. Particle size distribution profile as analysed by master sizer (Fig. 5) reveals the size distribution by volume (%). The yield, loading efficiency [loading efficiency % = (amount of drug in NPs/amount of drug loaded NPs) × 100] as well as drug entrapment efficiency [entrapment efficiency % = (amount of drug in NPs/initial amount of drug) × 100] of LTZ-loaded PLGA NPs were 77.44 ± 0.24, 14.34 ± 1.95 and 43.03 ± 2.20%, respectively. The zeta potential values of LTZ-loaded PLGA NPs were found to be negative, −12 to −19.50 mV.

LTZ and LTZ-loaded PLGA NPs were radiolabeled with ^{99m}Tc with high-labeling efficiency. The pertechnetate, which exists in heptavalent oxidation state, was added either to LTZ solution or to LTZ-loaded PLGA nanoparticle suspension and subsequently reduced to lower valence state by stannous chloride, resulting in the formation of the desired chelate at pH 3.75 in good yield. The major radiochemical impurities are free $^{99m}TcO_4^-$ and reduced hydrolysed technetium-99m. Radiolabeling was optimized under different experimental conditions involving the pH of the complex as well as concentrations of the drug and stannous chloride dihydrate.

The labeling efficiency and stability of labeled complex were ascertained by ascending thin layer chromatography. As the pH increased from 3 to 3.75 the radiolabeling efficiency also increased, from 73.4 to 93% and 78 to 94% in case of free LTZ and LTZ-loaded PLGA NPs, respectively (Table 1). However further increase in pH resulted in reduction in the labeling efficiency. The maximum labeling achieved for free LTZ and LTZ-loaded PLGA NPs was at pH 3.75.

The amount of stannous chloride used for reducing the pertechnetate played an important role in the labeling process (Table 2) The optimum amount of stannous chloride resulting in high labeling efficiency and low amount of radiocolloids was found to be 20 μg/ml for both free drug and nanoparticulate formulation. Lower amount of stannous chloride raised the concentration of unbound pertechnetate while higher amounts led to the formation of undesirable radiocolloids.

Table 3 represents the effect of incubation time on the labeling efficiency of the preparation containing stannous chloride, $^{99m}TcO_4^-$, and either free LTZ or LTZ-loaded PLGA NPs. The optimum incubation time period to attain high labeling efficiency was found to be 25 min.

The strength of binding of technetium to LTZ and LTZ-loaded PLGA NPs was determined by DTPA challenge study (Fig. 3). With increase in concentration (10–50 mM) of DTPA there was not much change in labeling efficiency in either preparation. At 50 mM concentration of DTPA the amount of transchelate was found to be less than 4% for both the free drug and the nanoparticulate formulation indicating the stability of the radiolabeled complexes.

Table 3
Effect of incubation time on the labeling efficiency of LTZ and LTZ-loaded PLGA NPs. Each value is the mean (± S.D.) of four experiments.

Incubation time (min)	% Radiolabeling	
	LTZ	LTZ-loaded PLGA NPs
0	79.13 ± 1.28	81.19 ± 1.01
10	83.25 ± 0.98	84.17 ± 0.88
15	85.38 ± 0.73	87.17 ± 0.71
20	90.66 ± 0.57	89.13 ± 0.39
25	94.16 ± 0.41	93.05 ± 0.31

Table 4 represents the data demonstrating the in vitro stability of ^{99m}Tc-labeled LTZ and LTZ-loaded PLGA NPs with time. The study continued upto 24 h, during which only 3–4.5% decrease in labeling efficiency was observed indicating the usefulness of the chelate for in vivo studies.

The in vivo stability of the chelates was further ascertained by performing the biodistribution studies in normal mice at 4 h post-injection time period and measuring the % injected dose (% ID) in various organs like heart, blood, liver, lung, spleen, mus-

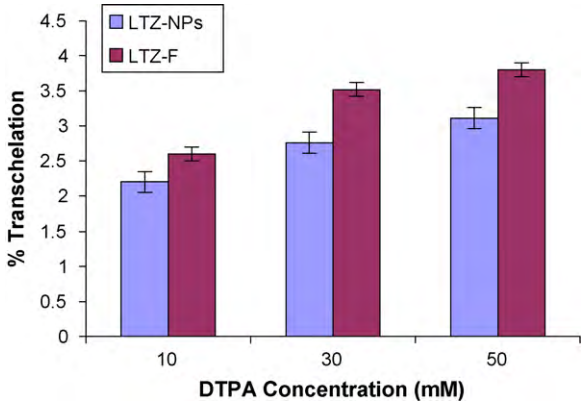

Fig. 3. Percent transchelation estimated by TLC, after mixing different molar concentration of DTPA with ^{99m}Tc-labeled free LTZ and LTZ-loaded PLGA NPs. Results are the mean and ± SEM of three separate experiments.

Table 4
In vitro Stability studies of LTZ and LTZ-loaded PLGA NPs in physiological saline and serum at 37 °C.

Time (h)	Percent radiolabeling			
	Saline		Serum	
	LTZ	LTZ-loaded PLGA NPs	LTZ	LTZ-loaded PLGA NPs
Initial	92.96 ± 0.47	93.85 ± 0.26	94.10 ± 0.22	93.38 ± 1.25
0.5	92.09 ± 0.96	92.15 ± 0.16	93.74 ± 0.45	93.12 ± 0.05
1	92.02 ± 0.18	91.58 ± 0.30	93.66 ± 0.35	92.49 ± 0.49
4	91.50 ± 0.38	90.91 ± 0.29	92.19 ± 1.37	91.15 ± 0.60
8	90.58 ± 0.38	89.62 ± 0.37	90.08 ± 0.13	89.62 ± 0.66
24	89.94 ± 0.74	89.60 ± 0.59	89.49 ± 0.62	89.35 ± 0.12

Each value is the mean (± S.D.) of four experiments.

Table 5
Biodistribution of ^{99m}Tc-labeled LTZ and LTZ-loaded PLGA NPs after intravenous injection in normal Swiss albino mice at 4 h post-injection.

Organ/tissue	LTZ	LTZ-loaded PLGA NPs
Liver	59.80 ± 0.65	47.80 ± 6.40
Lung	1.27 ± 0.04	1.04 ± 0.02
Spleen	1.78 ± 0.13	0.60 ± 0.04
Blood	2.68 ± 0.23	4.2 ± 0.51
Kidney	1.47 ± 0.13	1.70 ± 0.23
Intestine	4.98 ± 0.49	3.30 ± 0.04
Stomach	0.97 ± 0.05	0.68 ± 0.05
Urine	16.08 ± 1.21	4.53 ± 0.11
Heart	0.08 ± 0.00	0.09 ± 0.01
Muscle[a]	0.26 ± 0.02	0.15 ± 0.03

Results are expressed in percent-injected dose per organ/tissue (each value is the mean ± SEM of six mice).
[a] Percent-injected dose/g of tissue.

cle, kidney, stomach, and intestine (Table 5). To understand the anti-tumor activity of drug loaded PLGA NPs, biodistribution studies were undertaken in EA tumor bearing mouse models too. EAT cells were implanted in the right hind leg of the animal and the left leg was taken as control. The distribution of radioactivity in the above mentioned organs including tumors, after 1, 4, 8 and 24 h of intravenous injection of ^{99m}Tc-labeled free LTZ and LTZ-loaded PLGA NPs in tumor bearing mice is shown in Table 6.

^{99m}Tc-labeled free LTZ as well as LTZ-loaded nanoparticles exhibited significant hepatic uptake both in normal and tumor bearing mice model. In normal mice hepatic accumulation was comparatively higher with free drug (59.8% ID/organ.) than with the nanoparticulate suspension (47.8% ID/organ). Same pattern was noted in tumor model, however at 24 h LTZ-loaded nanoparticles exhibited higher hepatic uptake than that of free LTZ which could be attributed to slow blood clearance of the nanoparticulated formulation. Very low activity was found to clear by intestine, both in normal and in tumor models. Similarly kidney and heart uptakes were not very significant.

Renal clearance was significantly less for the nano-formulation (4.53%) than free LTZ (16.08%) in normal animal. In tumor model, renal clearance was low initially, 11.14 and 4.61% per organ at 1 h post-injection for ^{99m}Tc-labeled LTZ and LTZ-loaded PLGA NPs, respectively. This value moderately increased with time. At 24 h post-injection, renal clearance of LTZ and LTZ-loaded PLGA NPs was 28.6 and 20.3% ID/organ, respectively.

In normal animal, splenic uptake was not very high for both free drug and nano-formulation. In tumor model this value per organ was moderately high. The lung uptake of free LTZ and LTZ-loaded nanoparticles in normal mice was 1.27 and 1.04% per organ, respectively. In EA tumor bearing mice the uptake of free LTZ and LTZ-loaded nanoparticles by lung tissues was not very significant. Both for free drug and nanoparticles, very low overall radioactivity was recovered from the stomach of the normal as well as tumor bearing mice, indicating the in vivo stability of the ^{99m}Tc-labeled complexes.

In normal mice the blood activity of free drug was much less (2.68% ID/organ) than that of nanoparticles (4.2% ID/organ). In tumor model this value for free LTZ was 6.05% ID/organ initially but it sharply reduced with time (0.51% ID at 24 h), suggesting rapid blood clearance. However this was not observed in LTZ-loaded PLGA NPs, which exhibited blood activity of 2.70% ID/organ at 1 h reducing to 1.54% ID/organ at 24 h. This may be due to the sustained release of the drug from the nano-dispersion.

The tumor uptake of free LTZ was 0.35, 0.43, 0.33 and 0.26% ID/g of tumor tissue at 1, 4, 8 and 24 h post-injection, respectively. The tumor uptake of LTZ-loaded PLGA NPs was much better than that of free drug. At 1 h post-injection the above uptake was 0.47% ID/g which became remarkably significant at 4 h post-injection (1.99% ID/g); this was followed by slight decrease with time, 0.76 and 0.44% ID/g at 8 and 24 h post-injection, respectively.

Drug loaded nanoparticles exhibited much better tumor to muscle ratio than that of free letrozole, which was remarkably high, 3.73 at 4 h. The above value in case of free drug was 1.65. Scintigraphic images were obtained at 4 h after injecting ^{99m}Tc-labeled LTZ and LTZ-loaded PLGA NPs in tumor bearing mice. The uptake in tumor site was observable more predominantly in case of LTZ-loaded PLGA NPs (Fig. 4), however in both formulation significant

Table 6
Biodistribution of ^{99m}Tc-labeled LTZ-loaded PLGA NPs (LTZ-NPs), LTZ after intravenous injection in Swiss albino mice bearing Ehlrich Ascites tumor. Results are expressed in percent-injected dose per organ/tissue (each value is the mean ± SEM of six mice).

Organ/tissue	1 h		4 h		8 h		24 h	
	LTZ- NPs	LTZ	LTZ-NPs	LTZ	LTZ-NPs	LTZ	LTZ-NPs	LTZ
Urine	4.61 ± 0.41	11.14 ± 0.37	7.50 ± 0.3	14.99 ± 1.23	17.06 ± 0.34	20.11 ± 1.27	20.31 ± 0.43	28.6 ± 3.7
Kidney	0.50 ± 0.03	1.27 ± 0.25	0.87 ± 0.05	0.95 ± 0.05	0.65 ± 0.03	0.67 ± 0.01	0.56 ± 0.01	0.79 ± 0.21
Liver	52.03 ± 2.17	62.36 ± 2.01	47.92 ± 1.14	54.05 ± 0.9	44.73 ± 2.09	52.84 ± 3.5	42.74 ± 1.28	35.86 ± 0.84
Intestine	0.94 ± 0.05	4.77 ± 0.23	2.15 ± 0.30	5.17 ± 0.07	2.54 ± 0.27	6.42 ± 0.21	4.16 ± 0.23	11.34 ± 1.45
Stomach	0.29 ± 0.03	0.53 ± 0.09	0.48 ± 0.02	0.97 ± 0.16	0.45 ± 0.02	0.66 ± 0.07	0.34 ± 0.026	0.5 ± 0.08
Spleen	2.33 ± 0.21	4.12 ± 0.54	2.78 ± 0.27	3.95 ± 0.06	4.86 ± 0.26	0.26 ± 0.03	3.20 ± 0.21	0.27 ± 0.01
Lung	0.25 ± 0.01	0.86 ± 0.18	0.2 ± 0.02	0.36 ± 0.05	0.37 ± 0.01	0.28 ± 0.04	0.36 ± 0.01	0.20 ± 0.03
Blood	2.70 ± 0.31	6.05 ± 0.29	2.02 ± 0.26	1.69 ± 0.22	1.84 ± 0.17	1.25 ± 0.24	1.54 ± 0.07	0.51 ± 0.05
Tumor[a]	0.47 ± 0.06	0.35 ± 0.14	1.99 ± 0.19	0.43 ± 0.05	0.76 ± 0.04	0.33 ± 0.03	0.44 ± 0.03	0.26 ± 0.02
Muscle[a]	0.19 ± 0.03	0.27 ± 0.01	0.51 ± 0.06	0.26 ± 0.1	0.35 ± 0.02	0.21 ± 0.02	0.20 ± 0.01	0.17 ± 0.01

[a] Percent-injected dose/g of tissue.

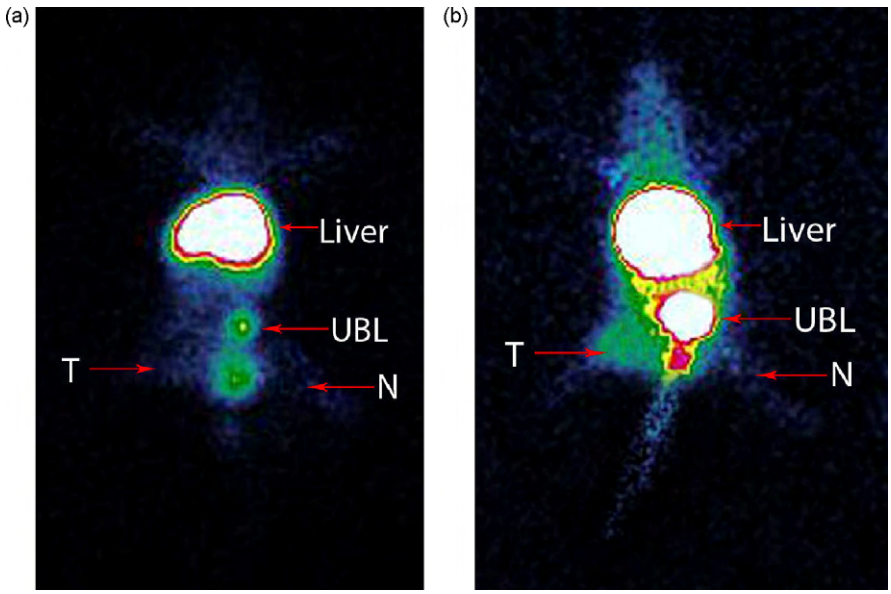

Fig. 4. Scintigraphic images of (a) normal and (b) Ehrlich Ascites tumor bearing mice at 4 h post-injection (i.v.) of ^{99m}Tc-labeled LTZ-loaded PLGA NPs. T = tumor cell implanted in right hind leg of mice, N = normal left hind leg.

amount of radioactivity was associated with urinary bladder and liver. Bladder activity cleared gradually with the increase of post-injection time period. All these are in concurrence with the results obtained from biodistribution studies.

4. Discussion

An important goal of cancer research is to formulate the drug in an efficient and safe delivery system that can selectively target the tumor cells with less systemic toxicity. In an attempt to target LTZ for breast cancer cells in case of postmenopausal women, LTZ was loaded into biodegradable PLGA polymers to facilitate controlled release of the drug from the nanodispersion for exerting sustained drug action, which could improve patient compliance. PLGA being a hydrophilic polymer may increase the circulation times of LTZ through avoidance of its removal by reticuloendothelial systems (RES). Direct precipitation technique produced spherical, relatively smooth surfaced nanoparticles (15–100 nm, Fig. 2). Master sizer analysis reveals the particle size distribution between 10 and 204 nm (Fig. 5). TEM analysis provides visual and descriptive information of a portion of whole population of the sample thus a clear picture of all the particles may not be obtained. Particle size plays an important role in improving the bioavailability of the drug loaded NPs. Smaller particles tended to accumulate in the tumor

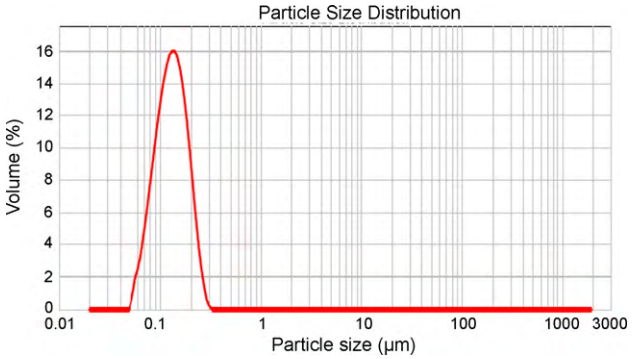

Fig. 5. A plot of particle size distribution of LTZ-loaded PLGA NPs by volume (%) estimated by master sizer 2000.

sites due to facilitated extravasation and greater internalization was also observed (Yuan et al., 1994). Smaller particles also make intravenous injection easier and their sterilization may be simply done by filtration (Konan et al., 2002). In addition, the smaller the size (~100 nm), the less will be the uptake by non-targeted cells as well as premature clearance by mononuclear phagocytic systems.

The presence of ionic stabilizer at the particle surface may influence the electrical charge distribution at the particle surface. Since poloxamer carries no electrical charge there is less influence on the surface charge of the particles. The negative zeta potential values could be attributed to the fact that free carboxyl groups from PLGA were deprotonated (distilled water, pH ~ 6.5) leading to a negatively charged polymer chain.

The use of technetium-99m has proven quite useful in understanding the in vivo fate of the drug loaded nanoparticulate formulation (Reddy et al., 2005; Halder et al., 2008). Radiolabeling was done under different pH condition to optimize the yield of radiolabeled free drug as well as drug loaded nano-dispersion. ^{99m}Tc-radiolabeling was undertaken with different amounts of stannous chloride to optimize parameters for maximum radiolabeling efficiency. The amounts of stannous chloride above the desired level results in undesirable radiocolloid formation and subsequent accumulation in the organs of RES due to macrophage uptake. However the concentration of stannous chloride below the optimum level leads to incomplete reduction of pertechnetate ($^{99m}TcO_4^-$) from its heptavalent state.

Stability of ^{99m}Tc-labeled LTZ and LTZ-loaded-PLGA NPs was studied in saline and in serum (rat) at 37 °C. Results revealed that there was hardly any decomposition of the label from the chelate. Even after a period of 24 h incubation the labeling efficiency was in the range of 89.3–90% indicating prolonged stability of the ^{99m}Tc-labeled preparation and the suitability of the complex for in vivo studies. Both ^{99m}Tc-labeled LTZ and LTZ-loaded-PLGA NPs exhibited negligible transchelation when incubated with DTPA solution of varying concentration, which indicates the strong binding of ^{99m}Tc with drug loaded NPs.

Variations in organ uptake and distribution were noticed between ^{99m}Tc-labeled free LTZ and LTZ-loaded PLGA NPs. The uptake of radiolabeled free LTZ in liver, lung and spleen, organs of RES at earlier time period, was comparatively higher than that of drug loaded NPs indicating the affinity of the free drug for these

organs. However, both free drug and drug-loaded nanodispersion exhibited much higher hepatic accumulation and slow clearance from liver. In contrast, urinary clearance was comparatively less; even after 24 h only 1/5th of the injected nano-dispersion was excreted through urine, though it was comparatively better in case of free drug (28% of injected dose excreted in 24 h). ^{99m}Tc-labeled free LTZ exhibited faster blood clearance than that of LTZ-loaded PLGA NPs. The blood concentration of drug-loaded nanoparticles at 24 h post-injection was three fold higher than that of free LTZ. This slow blood clearance of nanodispersion indicates long circulation capability. Increase in concentration of drug-loaded nanoparticles in tissues like spleen liver etc. could be attributed to its residence in blood for longer time. Prolonged circulation of nano-dispersion may improve the half-life of the drug and enhance its bioavailability. All these may result in infiltration of the drug molecule at greater concentration into the leaky endothelial cells of tumor sites due to increased microvascular permeability; subsequent accumulation in tumor tissue increased thereby. ^{99m}Tc-labeled LTZ-loaded PLGA NPs exhibited significantly high tumor uptake when injected intravenously in EA tumor bearing mice. The tumor uptake of drug-loaded NPs was almost 4.63-fold higher than that of free LTZ at 4 h post-injection. The higher tumor concentration of nanoparticles at 4 h post-injection was also confirmed by tumor imaging. Gamma image of mice exhibited significant uptake of ^{99m}Tc-labeled LTZ-loaded PLGA NPs in tumor region (right hind leg) than that of free LTZ (Fig. 4). Substantial uptake in the tumor region may render the recommendation of LTZ-loaded PLGA NPs for effective and prolonged tumor therapy.

5. Conclusion

LTZ-loaded PLGA NPs prepared by nanoprecipitation technique were radiolabeled efficiently with technetium-99m. These exhibited excellent in vitro stability (determined by DTPA challenge test) as well as very low stomach and intestinal concentration indicating in vivo stability of the formulation. The significantly high tumor uptake suggests the usefulness of the nanomatrix in the prolongation of the therapeutic efficacy of letrozole. Further investigations regarding the influence of administration route on the biodistribution and tumor uptake of LTZ-loaded PLGA NPs in tumor bearing mice model are under progress in this laboratory.

Acknowledgements

The authors are thankful to Dr. Aparna Laskar for her help in obtaining transmission electron micrograph. Financial support from the Council of Scientific and Industrial Research, New Delhi is gratefully acknowledged.

References

Allemann, E., Gurney, R., Doelker, E., 1993. Drug-loaded nanoparticles—preparation methods and drug targeting tissues. Eur. J. Pharm. Biopharm. 39, 173.

Allen, T.M., Hansen, C.B., Guo, L.S.S., 1993. Subcutaneous administration of liposomes: a comparison with the intravenous and intraperitoneal routes of injection. Biochim. Biophys. Acta 1150, 9–16.

Brannon-Peppas, L., 1995. Recent advances on the use of biodegradable micro particles and nanoparticles in controlled drug delivery. Int. J. Pharm. 116, 1–9.

Brigger, I., Dubernet, C., Couvreur, P., 2002. Nanoparticles in cancer therapy and diagnosis. Adv. Drug Deliv. Rev. 54, 631–651.

Brown, K., 2002. Breast cancer chemoprevention: risk-benefit effects of the antiestrogen tamoxifen. Expert Opin. Drug Saf. 1, 253–267.

Cohen, M.H., Johnson, J.R., Li, N., Chen, G., Pazdur, R., 2002. Approval summary: letrozole in the treatment of postmenopausal women with advanced breast cancer. Clin. Can. Res. 8, 665–669.

Dillen, K., Vandervoort, J., Mooter, G.V., Ludwig, A., 2006. Evaluation of ciprofloxacin-loaded Eudragit RS100 or RL100/PLGA nanoparticle. Int. J. Pharm. 314, 72–82.

Halder, K.K., Mandal, B., Chatterjee Debnath, M., Bera, H., Ghosh, L.K., Gupta, B.K., 2008. Chloramphenicol-incorporated poly lactide-co-glycolide (PLGA) nanoparticles: formulation, characterization, technetium-99m labeling and biodistribution studies. J. Drug Target. 16, 311–320.

Hughes, G.A., 2005. Nanostructure mediated drug delivery. Nanomedicine 1, 22–30.

Jain, R.A., 2000. The manufacturing techniques of various drug loaded biodegradable poly (lactide–co glycolide) (PLGA) devices. Biomaterials 21, 2475–2490.

Jin, C., Bai, L., Wu, H., Liu, J., Guo, G., Chen, J., 2008. Paclitaxel-loaded poly(D,L-lactide-co-glycolide) nanoparticles for radiotherapy in hypoxic human tumor cells in vitro. Cancer Biol. Ther. 7, 911–916.

Konan, Y.N., Gurney, R., Allemann, E., 2002. Preparation and characterization of sterile and freeze–dried sub-200 nm nanoparticles. Int. J. Pharm. 233, 239–252.

Long, B.J., Jelovac, D., Handratta, V., 2004. Therapeutic strategies using the aromatase inhibitor letrozole and tamoxifen in a breast cancer model. J. Natl. Cancer Inst. (Bethesda) 96, 456–465.

Mainardes, R.M., Evangelista, R.C., 2005. PLGA nanoparticles containing praziquantel: effect of formulation variables on size distribution. Int. J. Pharm. 290, 137–144.

Miller, W.R., 1997. Aromatase inhibitors in breast cancer. Cancer Treat. Rev. 23, 171–187.

Mondal, N., Pal, T.K., Ghosal, S.K., 2008. Development, physical characterization, micromeritics and in vitro release kinetics of letrozole loaded biodegradable nanoparticles. Pharmazie 63, 361–365.

Reddy, L.H., Sharma, R.K., Chutani, K., Mishra, A.K., Murthy, R.S.R., 2005. Influence of administration route on tumor uptake and biodistribution of etoposide loaded solid lipid nanoparticles in Dalton's lymphoma tumor bearing mice. J. Control. Release 105, 185–198.

Richardson, V.J., Jeyasingh, K., Jewkes, R.F., 1977. Properties of [^{99m}Tc] technetium labeled liposomes in normal and tumor bearing rats. Biochem. Soc. Trans. 5, 290–291.

Soppimath, K.S., Aminabhavi, T.M., Kulkarni, A.R., Rudzinski, W.E., 2001. Biodegradable polymeric nanoparticles as drug delivery devices. J. Control. Release 70, 1–20.

Vauthier, C., Dubernet, C., Chauvierre, C., Brigger, I., Couvreur, P., 2003. Drug delivery to resistant tumors: the potential of poly (alkyl cyanoacrylate) nanoparticles. J. Control. Release 93, 151–160.

Vogel, V.G., 2001. Reducing the risk of breast cancer with tamoxifen in woman at increased risk. J. Clin. Oncol. 19, 87S–92S.

Weir, H.K., Thun, M.J., Hankey, B.F., Ries, L.A.G., Howe, H.L., Wingo, P.A., Jemal, A., Ward, E., Anderson, R.N., 2003. Annual report to the nation on the status of cancer, 1975–2000, featuring the use of surveillance data for cancer prevention and control. J. Nat. Cancer Inst. (Bethesda) 95, 1276–1299.

Yamaguchi, K., Anderson, J.M., 1993. In vivo biocompatibility studies of medisorb 65/36 DL-lactide/glycolide copolymer microspheres. J. Control. Release 24, 81–93.

Yan, F., Zhang, C., Zheng, Y., Mei, L., Tang, L., Song, C., Sun, H., Huang, L., 2010. The effect of poloxamer 188 on nanoparticle morphology, size, cancer cell uptake, and cytotoxicity. Nanomed. Nanotech. Biol. Med. 6, 170–178.

Yuan, F., Leuning, M., Huang, S.K., Berk, D.A., Papahadjopoulos, D., Jain, R.K., 1994. Microvascular permeability and interstitial penetration of sterically stabilized (stealth) liposomes in human tumor xenograft. Cancer Res. 54, 3352–3356.